INTERNATIONAL JOURNAL of RENEWABLE ENERGY RESEARCH
K. Elatife et al., Vol.16, No.1, March, 2026

Performance Analysis of Rotor Blade Design Impact on OWC Impulse Radial Turbine

Khalid Elatife*‡, Abdellatif El Marjani**, Hamid Mounir***

* EMISys Research Team, E3S Research Center, Mohammed V University in Rabat, Mohammadia School of Engineers, Rabat, Morocco

**EMISys Research Team, E3S Research Center, Mohammed V University in Rabat, Mohammadia School of Engineers, Rabat, Morocco

***EMISys Research Team, E3S Research Center, Mohammed V University in Rabat, Mohammadia School of Engineers, Rabat, Morocco

(elatife@emi.ac.ma, elmarjani@emi.ac.ma, mounir@emi.ac.ma)

‡Corresponding Author; Khalid Elatife, Mohammadia School of Engineers, Mohammed V University, Avenue Ibn Sina, B.P. 765, Agdal, Rabat, Morocco, Tel: +212 613114720, elatife@emi.ac.ma

Received: 16.01.2024 Accepted:14.02.2024

Abstract- This study builds upon our previous numerical investigations by incorporating an extensive experimental validation of bi-directional radial impulse turbines used in oscillating water column (OWC) systems for wave energy conversion. Two rotor blade profiles, circular and elliptical, were analyzed to assess their influence on turbine performance under inhalation and exhalation modes. The combined computational fluid dynamics (CFD) simulations and experimental measurements provide detailed insights into flow angles, relative velocity distributions, and aerodynamic losses across turbine components, including the IGV, OGV, and rotor blades. Results confirm that circular blades deliver superior efficiency, particularly during inhalation, whereas elliptical blades exhibit significant local flow separation at the trailing edge. The enhanced experimental validation enables a more accurate assessment of the turbine's operational behavior. Finally, a control strategy for dynamically adjusting the geometric angles of guide vanes is proposed to optimize efficiency throughout the operating cycle. This work strengthens the understanding of rotor blade effects and provides a foundation for future intelligent control integration and design optimization in OWC turbines.

Keywords Bidirectional turbine, blade profile, wave energy extraction, performance analysis, flow separation.

Nomenclature

A_r	Turbine flow passage area ($= 2\pi R_r b$)	V	Absolute flow velocity
b	Blades height = 44 mm	V_r	Mean radial absolute flow velocity at R_r ($= \frac{Q_m}{\rho . A_r}$)
C_A	Pressure coefficient	V_u	Tangential absolute flow velocity
C_T	Torque coefficient	W	Relative velocity vector
P	Total pressure	α	Absolute flow angle
ΔP_0	Total pressure drop in the turbine	α^*	Geometrical angle of guide vanes
ΔP	Total pressure drop in a component	β	Relative flow angle
Q_m	Mass flow rate	η	Efficiency
R_c	Curvature radius	ζ	Loss coefficient
R_r	Mean radius of the rotor = 217mm	ρ	Air density
T	Turbine torque	ω	Angular speed = 234 rpm
U_r	Blade circumferential velocity at R_r	φ	Flow rate coefficient

1. Introduction

In recent times, a notable surge in attention regarding marine energy conversion has been remarked, particularly with regards to wave energy resources. The projected annual energy potential of this source is evaluated at about 32,000 TWh/yr [1]. As a result, significant research and development endeavors have been undertaken in the past few decades to effectively harness this energy [2], [3].

Artificial intelligence (AI) is increasingly used in renewable energy systems for performance optimization and intelligent control. Recent AI-driven smart grid studies demonstrate its potential to enhance technical efficiency in complex energy systems [4].

The oscillating water column (OWC) (Fig. 1-a) is considered as the most employed wave energy converter over the world. This can be attributed to several advantages, including accessibility, simplicity, and low maintenance costs [5]. The elements of an Oscillating Water Column (OWC) plant are illustrated in Fig. 1-b, comprising three primary segments: the air chamber which capture and transform wave energy into pneumatic form, the air turbine which converts this pneumatic energy into mechanical energy through a self-rectifying mechanism, and the electrical generator which converts the mechanical energy into electrical energy. Here, the efficiency of the entire energy conversion process hinges on the performance of each component, with a particular emphasis on the turbine, demanding substantial scrutiny [6].

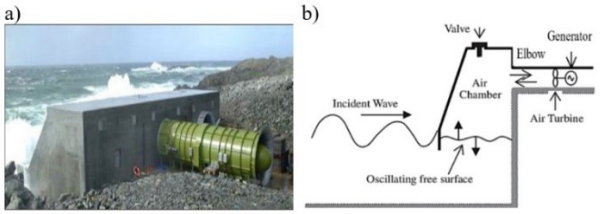

Fig. 1. The OWC system. LIMPET OWC plant in Scotland, UK [6] (a) and system description (b).

The bi-directional axial-flow Wells turbine, originally pioneered by Alan A. Wells in 1976 [8], has seen widespread adoption in numerous OWC installations. Furthermore, the bi-directional impulse turbine, which was designed and proposed by I.A. Babinstev in 1975 [9], has demonstrated its effectiveness as a solution for wave energy conversion within OWC devices. Although the air flow within the air chamber moves in both directions (inhalation and exhalation), both turbines demonstrate unidirectional rotation. Multiple turbine designs have been suggested and evaluated, as documented in references [10]–[12]. References [13], [14] contain a comparative study of the performance between impulse and Wells turbines, which highlights the high efficiency achieved by the Wells turbine. However, this kind of turbine suffers from certain shortcomings, including high efficiency within a limited flow rate range, inadequate starting characteristics, high noise levels, high-speed operation, elevated periodic axial thrust, and the issue of stall phenomenon. Despite extensive research carried out to address these shortcomings, the obtained results have not been significantly promising [14]–[16]. Hence, there has been a growing impetus in recent research to investigate alternative designs to the Wells turbine, notably the bi-directional impulse turbines.

Predominantly, research endeavors were directed towards the exploration of two distinct categories of impulse turbines, with their differentiation rooted in the configuration of rotor blades: axial turbines and radial turbines. A pair of guide vane assemblies, specifically the outer guide vanes (OGV) and the inner guide vanes (IGV), are strategically situated on either side of the rotor for improved flow guidance, as illustrated in Fig. 2. To further augment the efficiency of OWC devices, a twin configuration employing the impulse turbine was put forth as a potential solution for the axial disposition [17], [18], and for the radial disposition [19]. This approach involves the coupling of two turbines, each optimized to achieve optimal performance in either the inhalation or exhalation mode. Promising experimental results have demonstrated significant improvements in efficiency.

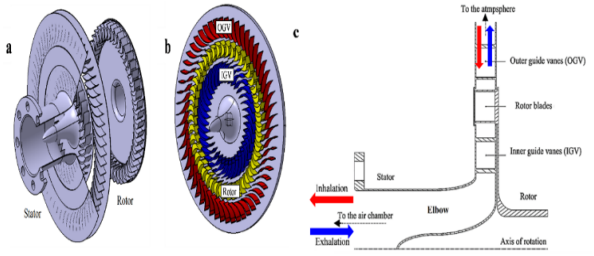

Fig. 2. Schematic representation of a radial impulse turbine in perspective view (a-b) and cross-sectional view (c).

The literature extensively acknowledges the pivotal role of blade profiles in determining turbine performance [21], [22]. Previous research efforts aimed at improving the performance of impulse turbines have predominantly focused on models based on elliptical profiles [12]. Nevertheless, Setoguchi et al. [23] have reported that blade profiles designed around circular shapes can exhibit notable efficiency. In an investigation conducted by Elatife and El Marjani, a research study examined the impact of circular and elliptical blade profiles on the average efficiency of a bi-directional radial impulse turbine [24]. The findings revealed a significant increase in efficiency for turbines with circular profiles compared to those with elliptical profiles. Such circular profiles contribute to minimizing pressure losses [25] and offer advantages in terms of design simplicity and manufacturing. However, there exists a noticeable gap in the literature according to comprehensive investigations into the impact of blade shape on the performance of air turbines equipping OWC systems.

This study builds upon our previous work [26]-[27], which presented a numerical evaluation of the global performance of two radial impulse turbines with circular and elliptical blades. In the present work, we extend that study by performing a more detailed experimental validation of the numerical model, providing additional data on flow behavior across various turbine components, including the fixed IGV and OGV blades and the rotor blades. The objective is to analyse the effect of the rotor blade profile on flow characteristics during directional changes (axial ↔ radial) and throughout the turbine components, with an emphasis on comparing computational predictions with experimental

measurements. CFD simulations were conducted using ANSYS Fluent to evaluate turbine performance, including geometric and flow angles at leading and trailing edges, loss coefficients, and relative velocity distributions in the inter-blade region. Finally, to optimize turbine efficiency throughout the operating cycle, we propose a control strategy for adjusting the geometric angles of the IGV and OGV in response to varying flow conditions, laying the groundwork for a future intelligent regulation system

2. Characteristics of the Turbine Design

The design attributes of the bidirectional radial impulse turbine are depicted in Fig. 2. A single rotor with symmetric blades accompanied by two stators composes the turbine. These stators incorporate rows IGV and OGV placed on both sides of the rotor blades (see Fig. 2-a and Fig. 2-b). Each set of guide vanes possesses the flexibility to operate as either inlet or outlet guide vanes, alternating their role depending on whether the incoming airflow is centripetal (inhalation mode) or centrifugal (exhalation mode) (see Fig. 2-c).

To assess their influence on turbine performance, two blade designs have been considered: one with circular profiles on the suction side and the other with elliptical profiles (referred to as TRC and TRE respectively). The TRC rotor blade design features on the pressure side a circular arc and on the suction side a combination of two straight lines and a circular arc (Fig. 3-a). In contrast, the TRE rotor blade design incorporates on the suction side an elliptical arc and on the pressure side a circular arc (Fig. 3-b). The design of the TRC rotor is rooted in the geometry of steam turbine rotors, as outlined in reference [28], and mirrors the identical geometrical shape studied in reference [29]- [30]. For the TRE rotor, all geometric parameters remain consistent with those of the circular rotor, except for the substitution of the circular profile on the pressure side with an elliptical profile. Importantly, the outlet and inlet blade angles remain identical (Fig. 3). Significantly, both types of rotors, circular and elliptical, maintain identical solidity, as the chord length and blade pitch were consistently preserved.

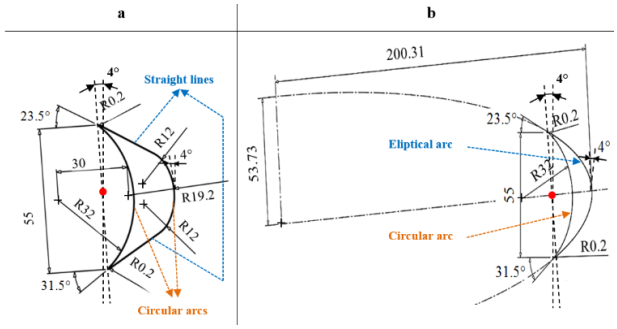

Fig. 3. Description of the geometrical characteristics of the two rotors: circular blades (a) and elliptical blades (b).

The turbine's fixed blades, including the OGV and IGV, feature circular arc designs on both pressure and suction sides. These guide vane dimensions are consistent for both TRC and TRE turbines, as illustrated in Fig. 4.

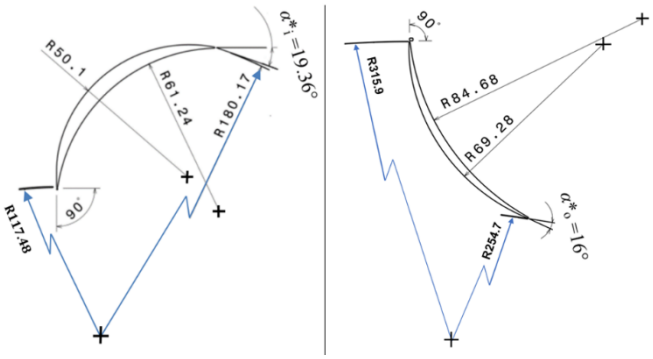

Fig. 4. IGV (left) and OGV (right) profiles.

The principal geometric features of the rotors in both TRC and TRE turbines are detailed in Table 1, as indicated below:

Table 1. primary geometric traits of turbine blades.

	Number of Blades	Geometrical angle (°)	Chord length (mm)	Solidity
IGV	32	α^*_i = 19.36	82	2.83
Rotor (TRC / TRE)	48	β^*_i = 31.5 /β^*_o= 23.5	55	1.93
OGV	64	α^*_o = 16	81	2.88

3. Computational Modeling

3.1. Working Flow Conditions

Numerical modeling is utilized to calculate shaft power across a range of flow coefficients (equation (1)) for both working modes of the turbine, specifically inhalation and exhalation. 3D numerical simulations using ANSYS Fluent 2021 R1 are used in order to assess the impact of blade profile on turbine performance. The flow is supposed to be incompressible, viscous, 3D, and steady. To optimize computational efficiency, periodic conditions were implemented in the computational domain (see Fig. 5) for reducing memory storage requirements. Periodic boundary conditions were implemented along the circumferential direction of the turbine, as illustrated in Fig. 5. Previous studies [6] have confirmed that using periodic domains allows accurate simulations without compromising accuracy. Given the turbine's composition, which includes both rotating and stationary components, the sliding mesh technique (SMM) was utilized to manage the relative motion between the fixed and rotating portions of the turbine. In the flow domain, an unstructured tetrahedral mesh was employed. The standard k-ε model has been employed to model the turbulent flow. For solving the flow equations for mass, momentum, and energy, a segregated solver has been used. The SIMPLEC approach is applied to ensure the pressure-velocity coupling. The discretization of the convection terms was achieved through the implementation of the high-order MUSCL scheme, while the diffusion terms were approximated using the classical central differences.

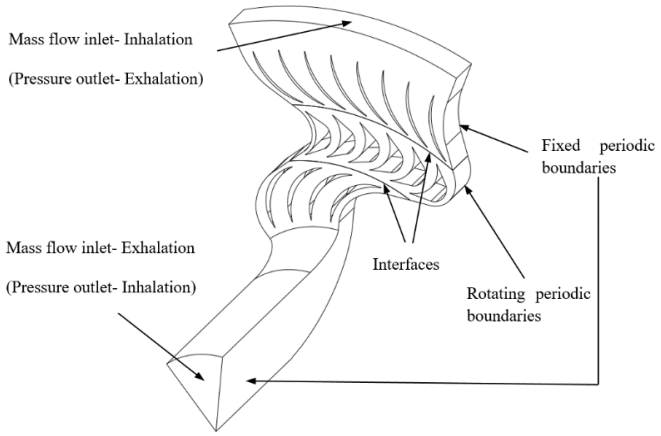

Fig. 5. Flow domain with periodic conditions.

In the exhalation mode, the chosen boundary conditions include at the inlet a uniform mass flow rate (Q_m) and at the outlet a uniform static pressure, which is atmospheric pressure. A fixed value of ω=234 rpm is assigned to the rotor's rotational velocity. The non-slip state is adapted to all stationary walls to account for shear condition. A radial equilibrium pressure distribution is implemented to ensure compatibility of the static pressure field in the pressure outlet boundary condition. Remaining configuration of the computational fluid dynamics (CFD) setup follows the default settings provided by the Ansys Fluent tool.

To ensure the accuracy of the results, a mesh convergence study was conducted, involving five different mesh refinements of the flow domain. The turbine efficiency (equation (2)) was calculated for each mesh refinement for both TRC and TRE turbines. The results of the grid independence study for TRC and TRE are presented in Fig. 6-a and -b, respectively. These figures indicate that the efficiency converges at approximately 4.5×10^6 cells for both turbines. Therefore, this mesh refinement was chosen for the subsequent simulations conducted in this analysis. Fig. 7 depicts the mesh details for the entire periodic flow domain of the turbine, as well as for the IGV, rotor, and OGV, as illustrated in Fig. 7-a, b, c, and d, respectively.

The working parameters for the investigated impulse turbine during steady-state conditions are as follows:

- Flow coefficient,

$$\varphi = V_r/U_r \quad (1)$$

- Turbine efficiency,

$$\eta_{turbine} = (T\omega)/(\Delta P_0(Q_m/\rho)) \quad (2)$$

Herein, U_r represents the circumferential velocity of the turbine blades, while V_r denotes the average radial flow velocity at the mean rotor radius, denoted as R_r. ΔP_0 represents the overall pressure differential existing between the turbine's inlet and outlet.

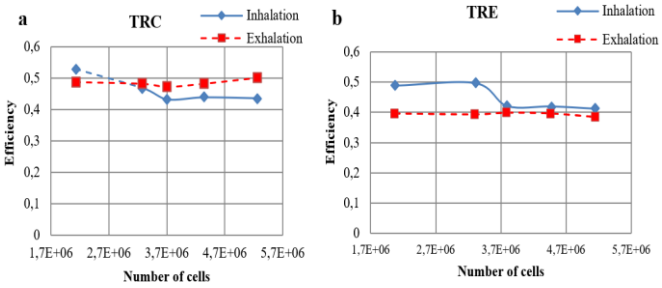

Fig. 6. Mesh independence study on the efficiency of TRC (a) and TRE (b).

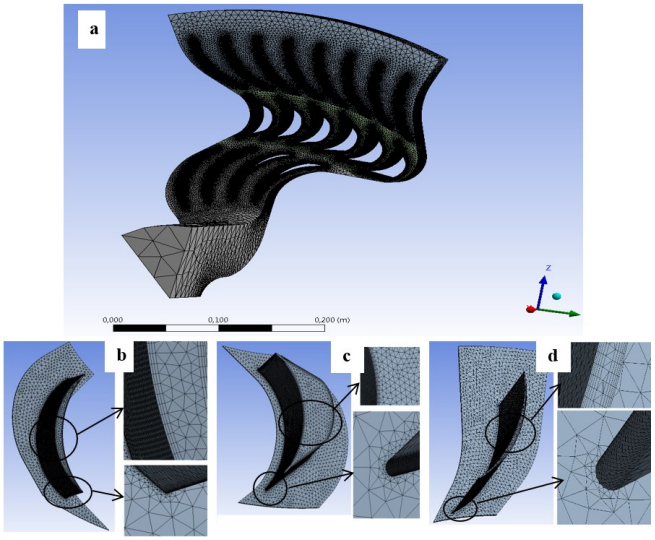

Fig. 7. Geometrical mesh: (a) Periodic flow domain of the turbine, (b) IGV blade mesh, (c) Rotor blade mesh and (d) OGV blade mesh.

3.2. Numerical Model Validation

The validation of the present CFD model is performed through a systematic comparison with the experimental data reported by Setoguchi et al. [29]. A schematic representation of the experimental impulse radial turbine is provided in Fig. 8, while Table 1 summarizes its principal geometrical characteristics. A comprehensive description of the turbine geometry can be found in the original publication by Setoguchi et al. [29].

The numerical simulations were conducted using the rotor configuration identified as Case (1) in the reference study. All computations were carried out with ANSYS Fluent, adopting the numerical setup and modeling assumptions detailed in the preceding section. In order to accurately reproduce the experimental configuration, a tip clearance of 1 mm between the rotating and stationary components was explicitly incorporated into the computational domain.

To ensure a consistent performance assessment under both centrifugal and centripetal operating modes, three dimensionless performance indicators were selected for comparison: the pressure coefficient C_A (equation. 3), the torque coefficient C_T (equation 4), and the mean efficiency $\bar{\eta}$ (equation 5). These parameters provide a comprehensive

evaluation of the turbine's aerodynamic behavior and energy conversion performance.

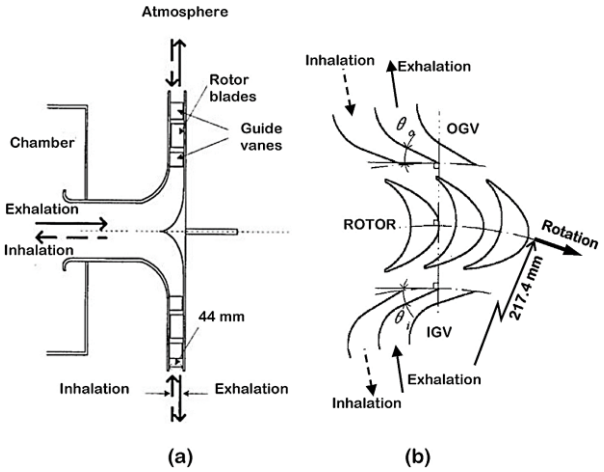

Fig. 8. Schematic representation of the impulse radial turbine experimentally investigated in [29].

Table 2. Principal geometrical parameters of the turbine configuration investigated experimentally in [29].

Components	Blade number	Chord length (mm)	Setting angle	Solidity
Inner guide vanes	52	50	θ_i= 25°	2.29
Rotor	51	54	Case 1 ([29])	2.02
Outer guide vanes	73	50	θ_o= 25°	2.28

Fig. 9 presents a direct comparison between the experimental measurements and the numerical predictions for the pressure coefficient (Fig. 9a), torque coefficient (Fig. 9b), and mean efficiency (Fig. 9c). Overall, a strong agreement is observed between the computational and experimental results, particularly in terms of trend evolution and order of magnitude. Minor discrepancies may be attributed to experimental measurement uncertainties, geometric simplifications, mesh discretization effects, and inherent numerical approximations associated with turbulence modeling.

Given the satisfactory level of agreement achieved, the present CFD model can be considered sufficiently accurate and robust for subsequent parametric investigations and optimization studies.

$$C_A = \frac{2\Delta P_0}{\rho(V_r^2 + U_r^2)} \quad (3)$$

$$C_T = \frac{2T}{\rho(V_r^2 + U_r^2)A_r R_r} \quad (4)$$

$$\bar{\eta} = (\eta_{\varphi=1} + \eta_{\varphi=-1})/2 \quad (5)$$

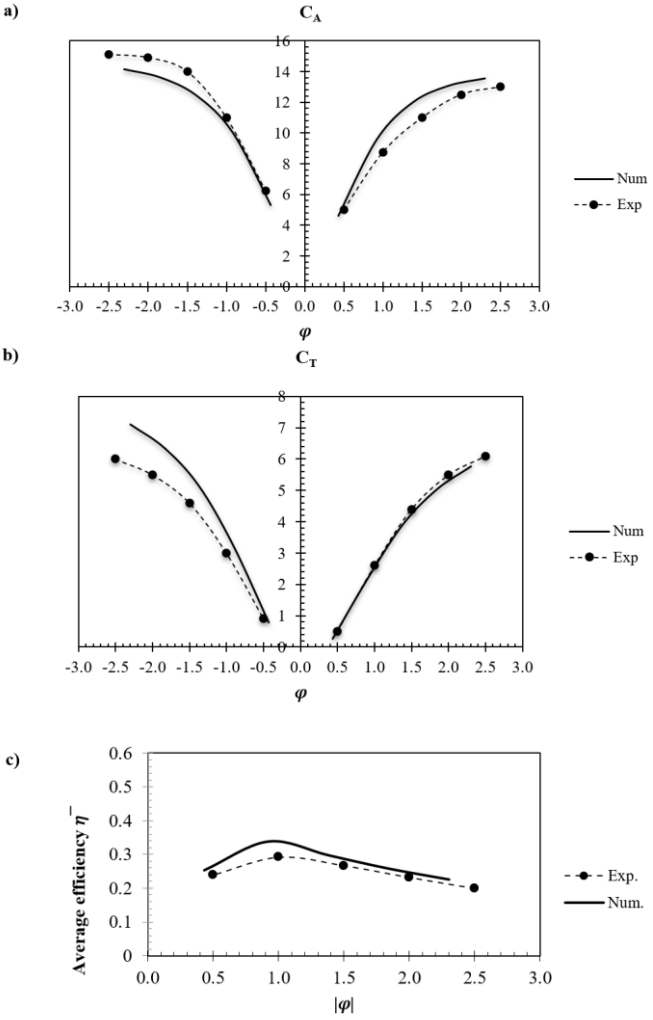

Fig. 9. Comparison between experimental data reported in [29] and present numerical predictions for the pressure coefficient (a), torque coefficient (b), and mean turbine efficiency (c).

4. Results and Analysis

4.1. Flow Angles Analysis

This section focuses on the analysis of flow behavior across the fixed and moving turbine blades. Initially, we examine the flow characteristics in two turbine configurations, TRC and TRE, by analyzing the variations in flow angles at stations B, C, D, and E at the leading and trailing edges of the blades, as illustrated in Fig. 10. A comparison is made between the flow and geometrical angles. For the fixed element stations (B and E), the flow absolute angle (α) represents the angle between the tangential direction and the absolute velocity vector V. At stations C and D related the rotor, the relative flow angle (β) is considered, representing the angle between the tangential direction and the relative velocity vector W. The angles α^* and β^* denote the respective geometrical angles of the fixed elements (IGV and IGV) and the rotor, as indicated in Fig. 11.

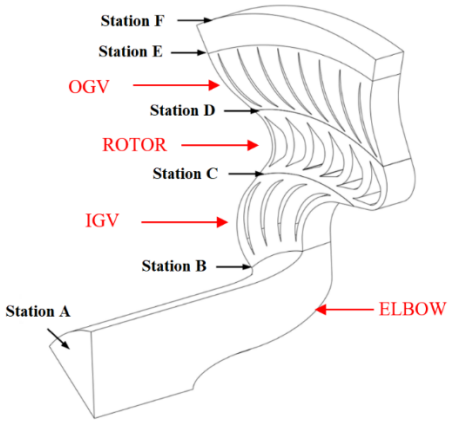

Fig. 10. Different reference stations in the flow domain of the turbine.

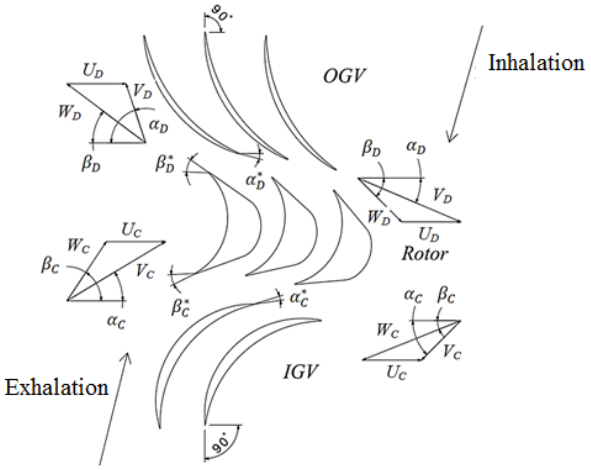

Fig. 11. Flow angles (α, β) and geometrical angles (α^*, β^*).

- Case on inhalation mode: Fig. 12-a to -d

The variations of flow angles with the flow coefficient are nearly identical in both turbine configurations, except at station C, which corresponds to the IGV leading edge, where a difference of 10° is observed. At this specific station, the flow direction favors the TRC configuration as the flow angle closely aligns with the blade's geometrical angle. Significant disparities between flow and geometric angles can be observed, particularly pronounced at low flow coefficients. These angle differences can be attributed to boundary layer separation caused by changes in blade curvature, leading to increased aerodynamic losses and reduced efficiencies. On the other hand, it seems that the geometrical angle at the leading edge of the rotor blade is correctly matched with the flow angle.

- Case of exhalation mode: Fig. 12-e to -h

The flow angles variations with the flow coefficient are practically the same in both turbine configurations, but at the all stations unlike the inhalation mode. Significant variations are noticeable at the leading edge of the OGV blades, and this is a result of the boundary separation occurring at the trailing edge of the rotor blades. From these results, it can be expected that both turbines would have, practically, the same performances.

The variations of flow angles with the flow coefficient are similar in both turbine configurations, except in the inhalation mode where differences arise at all stations. Notably, significant disparities occur at the leading edge of the OGV caused by boundary separation at rotor's blade trailing edge. Based on these findings, it can be anticipated that both turbines would exhibit comparable performances.

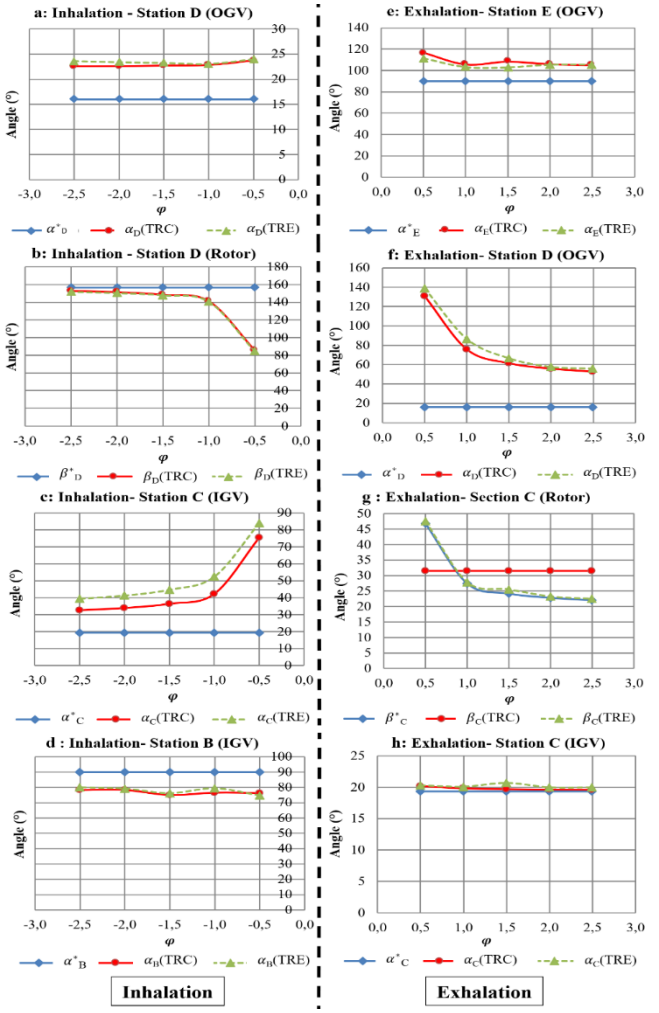

Fig. 12. Flow angle variations at stations B, C, D and E; for inhalation: a, b, c and d, and for exhalation: e, f, g and h.

4.2. Analysis of Aerodynamic Losses

In order to analyze the aerodynamic losses within the turbine elements, including the Elbow, stator (IGV and OGV) and Rotor, two phases of work are conducted. This examination aims to enhance our comprehension of the loss mechanisms linked to the 3D viscous flow characteristics within the turbine design.

In this respect, the loss coefficient ζ in fixed turbine elements (Elbow, IGV and OGV) was evaluated with following relations:

	Exhalation	Inhalation
Elbow	$\zeta_{elbow}^{exh} = \frac{(P_A - P_B)}{0.5\rho V_A^2}$ (4a)	$\zeta_{elbow}^{inh} = \frac{(P_B - P_A)}{0.5\rho V_B^2}$ (4b)
IGV	$\zeta_{IGV}^{exh} = \frac{(P_B - P_C)}{0.5\rho V_B^2}$ (5a)	$\zeta_{IGV}^{inh} = \frac{(P_C - P_B)}{0.5\rho V_C^2}$ (5b)
OGV	$\zeta_{OGV}^{exh} = \frac{(P_D - P_E)}{0.5\rho V_D^2}$ (6a)	$\zeta_{OGV}^{inh} = \frac{(P_E - P_D)}{0.5\rho V_E^2}$ (6b)

With V_i is the inlet absolute velocity for each component at the zone 'i' (**Hata! Başvuru kaynağı bulunamadı.**).

The results are shown in Fig. 13-a, -b and -c, respectively, for the elbow, the IGV and the OGV at different flow coefficients. For the inhalation mode, high losses are encountered in the elbow (Fig. 13-a) and the IGV (Fig. 13-b). While in the exhalation mode the highest level is obtained in the OGV component. All results are in accordance with those obtained in the total pressure drop analysis and the flow angle analysis. Results confirm again that the TRC configuration is more efficient than the TRE one. Low losses levels are noticed in all cases with circular design.

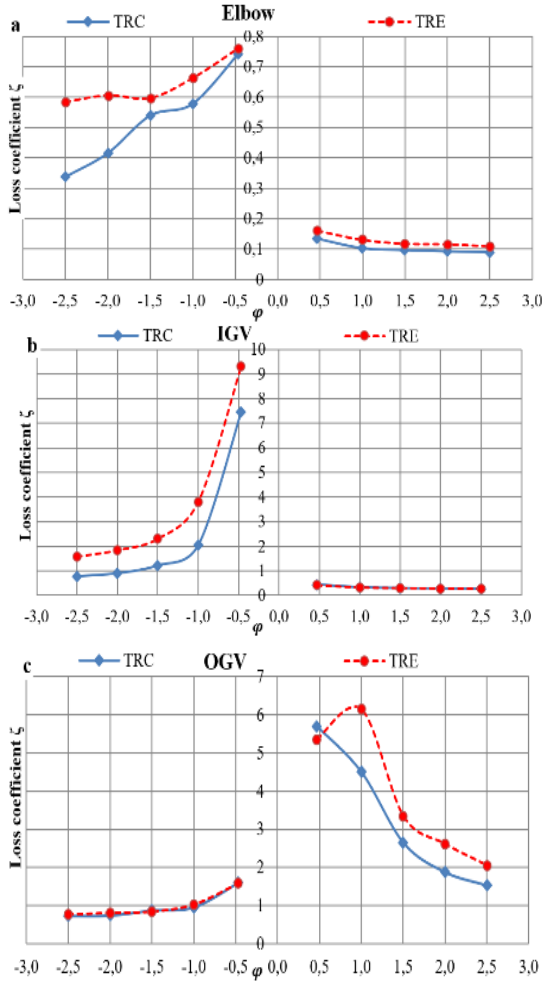

Fig. 13. Loss coefficient for the elbow (a), inner guide vanes (b) and outer guide vanes (c).

4.3. Rotor Blade Flow Analysis

The relative flow in the inter-blade passage for both turbine configurations; circular and elliptical is analysed in this section. The relative flow streamlines over the blade's surfaces are considered in order to evaluate how the flow is guided and the behaviour of the boundary layer. Analyses are conducted at the flow coefficient φ of 1, revealed from the efficiency comparisons as the most efficient point. Streamlines results for the case of inhalation and exhalation modes are presented in Fig. 14 and Fig. 15 respectively. Flow patterns indicate good concordance between the flow direction and the blade deviation in the area of the blade leading edge. However, large flow disturbances can be noticed particularly at the blade trailing edge where flow separation appears, deteriorating the flow guidance and leading to the large differences between flow and blade angles indicated in Fig. 12 This behaviour affects also the losses in the turbine as has been confirmed previously in Fig. 13. Comparisons between the TRC and the TRE configurations indicate that the flow separation is more pronounced in the later configuration.

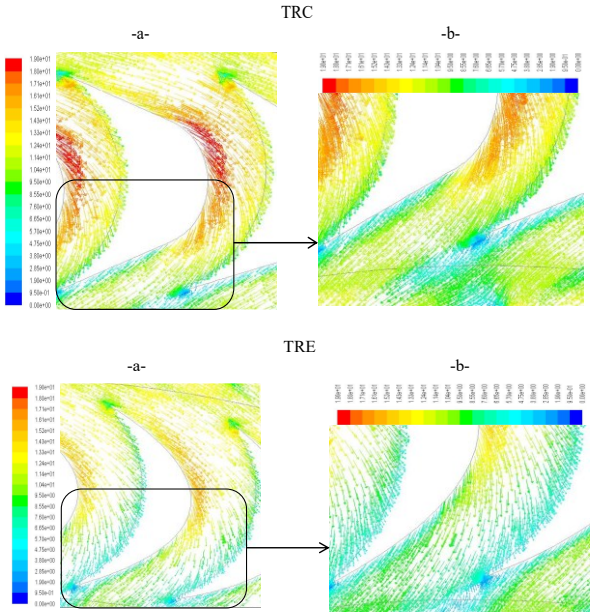

Fig. 14. TRC (up) and TRE (down) velocity fields in inhalation mode - (a) Inter-blade passage and (b) Trailing edge area.

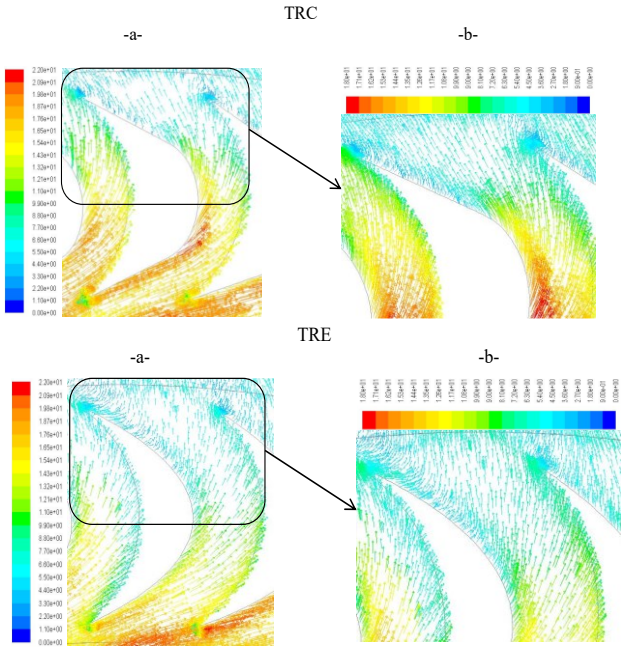

Fig. 15. TRC (left) and TRE (right) velocity fields in exhalation mode - (a) Inter-blade passage and (b) Trailing edge area.

The flow separation phenomenon is related to curvature variation of the blade surface. Fig. 16 gives the blades curvature variation along the radial direction for both blade configurations. The elliptical profile exhibits a significant variation in the radius of curvature, whereas the circular profile maintains a constant radius of curvature. Based on this comparison, the boundary layer separation can be anticipated and is more likely to occur with the elliptical profile than with the circular one.

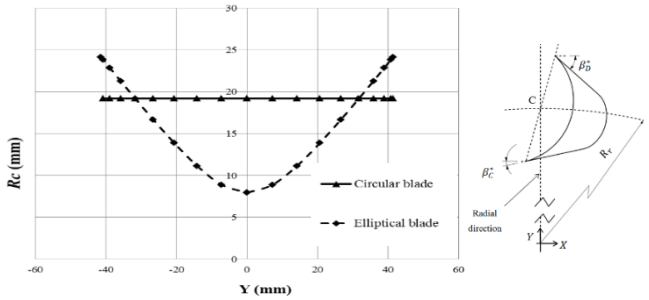

Fig. 16. Curvature radius (R_c) variation with the radial direction Y.

5. Intelligent System for Further Improvement

Following the angle study carried out in a previous part of this paper, it can be noticed that the guide vanes downstream of the rotor during both flow modes; OGV for exhalation and IGV for inhalation, show a mismatch between their geometric angles and the flow angle. Otherwise α_D^* differs from α_D for all flow coefficients during exhalation (Fig. 12-f), and α_c^* and α_c during inhalation (Fig. 12- c). This mismatch causes considerable losses (Fig. 13), so finding a solution to ensure the right angles (geometric and flow) for the guide vanes will boost turbine efficiency considerably.

To achieve this, we propose an intelligent system that will control the permanent matching of the geometric angles of the guide vanes (IGV and OGV) with the variation in flow angle during both inhalation and exhalation modes. This system is illustrated in Fig. 17. The system consists of installing a bidirectional flow meter in the OWC air chamber, and depending on the flow value, an integrated processing unit will calculate the corresponding geometrical angle according to the velocity triangle principle, and send a command to the servomotors. The latter, which are coupled to the axes of the guide vanes (IGV or OGV), will drive their rotation. a detailed study of this system will be the subject of future work.

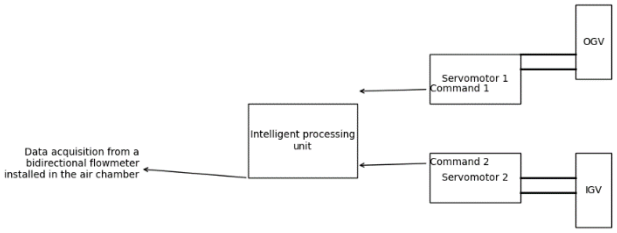

Fig. 17. Description of the proposed intelligent system for improving the turbine performance.

6. Conclusion

This study extends previous numerical investigations of radial impulse turbines in OWC wave energy converters by incorporating a more comprehensive experimental validation of both circular and elliptical rotor blade profiles. The combined numerical and experimental analyses provide a deeper insight into flow behavior within turbine components, including the IGV, OGV, and rotor blades, under both inhalation and exhalation modes. Results confirm that circular blades offer superior performance, particularly in inhalation mode, while elliptical blades exhibit significant local flow separation due to their higher curvature. The detailed experimental data allow a more accurate assessment of flow angles, relative velocity distributions, and loss coefficients across the turbine components. Building on these findings, a control strategy for dynamically adjusting the geometric angles of guide vanes is proposed to optimize turbine efficiency throughout the operating cycle. This work provides a more robust foundation for future studies aiming to integrate intelligent control systems and improve the design and performance of OWC turbines.

Acknowledgements

This research work has been conducted as part of the research activity within the EMISys research team with the support of Mohammadia School of Engineers and Mohammed V University in Rabat, Morocco.

Author Contributions

K. Elatife Conceptualization, K. Elatife; methodology and supervision, A. El Marjani; investigation and validation, K. Elatife; data curation and formal analysis, K. Elatife;

writing—original draft preparation, K. Elatife and H. Mounir; writing—review and editing, H. Mounir and A. El Marjani; all authors have read and agreed to the published version of the manuscript.

Conflict of Interest

The author(s) declared no potential conflicts of interest with respect to the research, authorship, and/or publication of this article.

References

[1] Y. Wen and Y. M. Low, "Long-term resource assessment and decarbonization potential of wave energy", Renewable Energy, 2025, doi: 10.1016/j.renene.2025.124287.

[2] T. Aderinto and H. Li, "Ocean wave energy converters: Status and challenges", Energies, vol. 11, no. 5, 2018, doi: 10.3390/en11051250.

[3] N. Guillou, G. Lavidas, and G. Chapalain, "Wave energy resource assessment for exploitation—A review", Journal of Marine Science and Engineering, vol. 8, no. 9, p. 705, September 2020, doi: 10.3390/jmse8090705.

[4] D. Clemente, P. Rosa-Santos, and F. Taveira-Pinto, "On the potential synergies and applications of wave energy converters: A review", Renewable and Sustainable Energy Reviews, vol. 135, p. 110162, January 2021, doi: 10.1016/j.rser.2020.110162.

[5] H.N. Senyapar and R. Bayindir, "AI-driven smart grid solutions for energy justice: Integrating technical efficiency with inclusive social welfare policy design", International Journal of Smart Grid, vol. 9, no. 3, pp. 105–115, 2025, doi: 10.20508/ijsmartgrid.v9i3.426.g400.

[6] A.F. Falcão, "Overview on oscillating water column devices", Floating Offshore Energy Devices: GREENER, vol. 20, no. 1, 2022.

[7] A. El Marjani, F. Castro Ruiz, M.A. Rodriguez, and M. T. Parra Santos, "Numerical modelling in wave energy conversion systems", Energy, vol. 33, no. 8, pp. 1246–1253, 2008, doi: 10.1016/j.energy.2008.02.018.

[8] A.F.O. Falcão and J.C.C. Henriques, "Oscillating-water-column wave energy converters and air turbines: A review", Renewable Energy, vol. 85, pp. 1391–1424, January 2016, doi: 10.1016/j.renene.2015.07.086.

[9] A.A. Wells, "Fluid driven rotary transducer", US Patent 1595700, 1980.

[10] I.A. Babinstev, "Apparatus for converting sea wave energy into electrical energy", US Patent 3922739, 1975.

[11] A.F.O. Falcão and L.M.C. Gato, "Air turbines", in Comprehensive Renewable Energy, vol. 8, 2012, doi: 10.1016/B978-0-08-087872-0.00805-2.

[12] P. Halder, M.H. Mohamed, and A. Samad, "Wave energy conversion: Design and shape optimization", Ocean Engineering, vol. 150, pp. 337–351, 2018, doi: 10.1016/j.oceaneng.2017.12.072.

[13] T. Setoguchi and M. Takao, "Current status of self-rectifying air turbines for wave energy conversion", Energy Conversion and Management, vol. 47, no. 15–16, pp. 2382–2396, 2006, doi: 10.1016/j.enconman.2005.11.013.

[14] A. Thakker, P. Frawley, H. B. Khaleeq, and E. S. Bajeet, "Comparison of 0.6 m impulse and Wells turbines for wave energy conversion under similar conditions", Proc. 11th International Offshore and Polar Engineering Conference, Stavanger, Norway, 2001.

[15] M. Takao, S. Fukuma, S. Okuhara, M. M. A. Alam, and Y. Kinoue, "Performance comparison of turbines for bi-directional flow", IOP Conference Series: Earth and Environmental Science, vol. 240, no. 5, p. 052002, March 2019, doi: 10.1088/1755-1315/240/5/052002.

[16] P. Halder, S. Hyung, and A. Samad, "Numerical optimization of Wells turbine for wave energy extraction", International Journal of Naval Architecture and Ocean Engineering, vol. 9, no. 1, pp. 11–24, 2017, doi: 10.1016/j.ijnaoe.2016.06.008.

[17] T.K. Das, E. Kerikous, N. Venkatesan, G. Janiga, D. Thevenin, and A. Samad, "Performance improvement of a Wells turbine through an automated optimization technique", Energy Conversion and Management: X, vol. 16, p. 100285, December 2022, doi: 10.1016/j.ecmx.2022.100285.

[18] A.T.M. Kotb, M.A.A. Nawar, Y.A. Attai, and M.H. Mohamed, "Performance optimization of a modified Wells turbine for wave energy conversion", Ocean Engineering, vol. 280, p. 114849, July 2023, doi: 10.1016/j.oceaneng.2023.114849.

[19] M. Takao and T. Setoguchi, "Air turbines for wave energy conversion", ISRN Renewable Energy, 2012, doi: 10.1155/2012/717398.

[20] V. Jayashankar, S. Anand, T. Geetha, S. Santhakumar, V. Jagadeesh Kumar, M. Ravindran, T. Setoguchi, M. Takao, K. Toyota, and S. Nagata, "A twin unidirectional impulse turbine topology for OWC based wave energy plants", Renewable Energy, vol. 34, no. 3, pp. 692–698, March 2009, doi: 10.1016/j.renene.2008.05.028.

[21] N. Ansarifard, A. Fleming, A. Henderson, S. Kianejad, and S. Chai, "Design optimisation of a unidirectional centrifugal radial-air-turbine for application in OWC wave energy converters", Energies, vol. 12, no. 14, 2019, doi: 10.3390/en12142791.

[22] B. Pereiras, F. Castro, A. El Marjani, and M. A. Rodríguez, "An improved radial impulse turbine for OWC", Renewable Energy, vol. 36, no. 5, pp. 1477–1484, 2011, doi: 10.1016/j.renene.2010.10.013.

[23] J. Ramarajan and S. Jayavel, "Performance improvement in Savonius wind turbine by modification of blade shape", Journal of Applied Fluid Mechanics, vol. 15, no. 1, pp. 99–107, 2021, doi: 10.47176/JAFM.15.01.32516.

[24] T. Setoguchi, "A review of impulse turbines for wave energy conversion", International Journal of Rotating Machinery, vol. 23, pp. 261–292, 2001.

[25] K. Elatife and A. El Marjani, "Efficiency improvement of a self-rectifying radial impulse turbine for wave energy conversion", Energy, vol. 189, 2019, doi: 10.1016/j.energy.2019.116257.

[26] O. Uzol and C. Camci, "Heat transfer, pressure loss and flow field measurements downstream of staggered two-row circular and elliptical pin fin arrays", Journal of Heat Transfer, vol. 127, no. 5, p. 458, 2005, doi: 10.1115/1.1860563.

[27] K. Elatife and A. El Marjani, "Blade profile effect on the impulse radial turbine performances for OWC wave energy converter", Lecture Notes in Networks and Systems, vol. 714, pp. 149–161, 2023, doi: 10.1007/978-3-031-35245-4_14.

[28] K. Elatife and A. El Marjani, "Numerical investigation and new intelligent system for performance improvement of a radial impulse turbine for wave energy conversion", International Journal of Energy for a Clean Environment, vol. 26, no. 1, 2025, doi: 10.1615/InterJEnerCleanEnv.2024051511.

[29] F.R. Harris, "The Parsons centenary—A hundred years of steam turbines", Proceedings of the Institution of Mechanical Engineers, vol. 198, no. 3, pp. 183–224, 1984, doi: 10.1243/PIME_PROC_1984_198_024_02.

[30] K. Elatife and A. El Marjani, "Optimization design procedure of a radial impulse turbine in OWC system", International Energy Journal, vol. 18, no. 4, pp. 365–378, 2018.

[31] T. Setoguchi, S. Santhakumar, M. Takao, T. H. Kim, and K. Kaneko, "A performance study of a radial turbine for wave energy conversion", Proceedings of the Institution of Mechanical Engineers, vol. 216, pp. 15–22, 2002.